

Coupled core-edge simulations of H-mode buildup using the Fusion Application for Core-Edge Transport Simulations (FACETS) code

A. H. Hakim,^{1,a)} T. D. Rognlien,² R. J. Groebner,³ J. Carlsson,¹ J. R. Cary,¹ S. E. Kruger,¹ M. Miah,¹ A. Pankin,¹ A. Pletzer,¹ S. Shasharina,¹ S. Vadlamani,¹ R. Cohen,² and T. Epperly²

¹*Tech-X Corporation, 5621 Arapahoe Ave. - Suite A Boulder, Colorado 80305, USA*

²*Lawrence Livermore National Laboratory, Livermore, CA 94551, USA*

³*General Atomics, PO Box 85608, San Diego, CA 92186-5608, USA*

(Received 25 October 2011; accepted 16 February 2012; published online 16 March 2012)

Coupled simulations of core and edge transport in the DIII-D shot number 118897, after the L-H transition but before the first edge localized mode (ELM), are presented. For the plasma core transport, a set of one dimensional transport equations are solved using the FACETS:Core solver. The fluxes in this region are calculated using the GLF23 anomalous transport model and Chang-Hinton neoclassical model. For the plasma edge transport, two-dimensional transport equations are solved using the UEDGE code. Fluxes in the edge region use static diffusivity profiles based on an interpretive analysis of the experimental profiles. Simulations are used to study the range of validity of the selected models and sensitivity to neutral fueling. It has been demonstrated that the increase of neutral influx to the level that exceeds the level of neutral influx obtained from analysis simulations with the UEDGE code by a factor of two results in increased plasma density pedestal heights and plasma density levels in the scrape-off-layer region. However, the additional neutral influx has relatively weak effect on the pedestal width and plasma density profiles in the plasma core for the DIII-D discharge studied in this research. © 2012 American Institute of Physics.

[<http://dx.doi.org/10.1063/1.3693148>]

I. INTRODUCTION

Predictive modeling of tokamak plasmas has traditionally treated the plasma core and plasma edge regions separately. The core region that is characterized by closed field-lines and hot, fully ionized plasmas. The edge region is characterized by the change of magnetic topology and lower temperature plasmas. In the hotter core region, the transport parallel to the magnetic field lines is much larger comparing to the transport that is perpendicular to the magnetic field lines. On the open-field lines, the rapid parallel motion gives rise to a boundary layer near the separatrix, in both the open and closed field line region, where the parallel and perpendicular transport compete and the transport is two-dimensional and cannot be treated with 1D model. The plasma fueling of the plasma via neutrals from the walls also can strongly influence the two-dimensional nature of this boundary layer region. Thus, the edge region includes the closed field line region near the separatrix where the plasma quantities are two-dimensional. The extent of the edge region that contains closed field lines will depend on the plasma parameters determining the parallel equilibration that makes the quantities one-dimensional.

Computational modeling of the core region has benefited from the development and use of one-dimensional transport equations^{1,2} suitable for modeling of the plasma on long time scales. The core transport equations serve as the dominant paradigm for analysis of experiments, design of future machines, and understanding core transport. Sophisticated

computational models for the sources; e.g., neutral-beam³ or radio frequency;⁴ and transport fluxes; e.g., anomalous⁵ or neoclassical⁶ have been developed with the interfaces provided by this one-dimensional transport paradigm. This effort has been reasonably successful in providing the capability of being predictive; i.e., modeling plasmas over long time scales with minimal input of free parameters.

The edge region has also developed transport equations for simulations that resolve transport time scales.⁷ Judicious use of the edge transport codes in conjunction with experimental constraints has allowed many features of tokamak edge plasmas to be studied including the heat loads on the divertors⁸ and divertor detachment.⁹ However, a complete predicted understanding of edge physics is currently lacking.

Although transport modeling for each individual region is well-established, transport simulations of the whole region are less frequently performed. Two approaches for modeling the entire region are available. The first is to extend the edge codes all the way into the core and perform two-dimensional modeling over the entire region. This approach is difficult because the fast parallel equilibration time scale must be included and even with implicit methods significant computational challenges are introduced. More critically, any efforts to reuse the flux and source models, which were frequently written for interfacing to one-dimensional transport codes, must undertake significant additional work to reuse those components. Concordantly, the fusion application for core-edge transport simulations (FACETS) project¹⁰ has followed a different approach and models model each region separately and couple them together.

^{a)}Permanent address: Princeton Plasma Physics Laboratory, P.O. Box 451, Princeton, NJ 08543-0451. Electronic mail: ammar@princeton.edu.

In this paper, we present results from coupled FACETS core-edge (CE) simulations of pedestal buildup in the DIII-D tokamak for a selected shot. The rest of the paper is organized as follows. The core and edge equations that are used in the analysis are described along with the coupling scheme to advance the coupled system self-consistently in time. In Sec. III, the experimental discharge studied (DIII-D shot 118897) and the initial conditions and edge interpretive analysis used in the calculations are described. Results are presented and discussed. Section IV shows the impact of gas-puff on plasma profile evolution. Finally, conclusions are discussed.

II. CORE AND EDGE MODELS AND COUPLING SCHEME

In this set of simulations, the following equations are solved for the core region:

$$\frac{\partial n}{\partial t} + \frac{1}{V'} \frac{\partial}{\partial \rho} (V' F_n^\rho) = S_n, \quad (1)$$

$$\frac{3}{2} \frac{\partial}{\partial t} (n T_s) + \frac{1}{V'} \frac{\partial}{\partial \rho} (V' F_s^\rho) = S_s, \quad (2)$$

where $n(\rho, t)$ is the plasma number density, $T_s(\rho, t)$ are electron ($s = e$) and ion ($s = i$) temperatures, F_n^ρ is the contravariant particle flux, F_s^ρ are the contravariant thermal fluxes, and $S_n(\rho, t)$ and $S_s(\rho, t)$ are the particle and thermal sources. The independent variable is the dimensionless normalized toroidal flux ρ and the geometry is encapsulated in $V' \equiv dV/d\rho$, where $V(\rho)$ is the volume enclosed inside the flux surface ρ . These equations are a subset of the full set of transport equations.^{1,2} Specifically, we have assumed that the changes in magnetic geometry are negligible over the time scale of our simulation, and that the effect of impurities can be sufficiently modeled using a Z_{eff} profile to obtain their effects on the fluxes, radiation losses, and temperature equilibration.

The fluxes are computed using a combination of anomalous and neoclassical terms $F_{\text{GLF}} + F_{\text{CH}} + F_{\text{ETG}}$, where F_{GLF} is the anomalous flux computed using the GLF23 (Ref. 11) model, F_{CH} is the neoclassical flux computed using the Chang-Hinton⁶ model, and F_{ETG} (ETG, Electron Temperature Gradient) is anomalous electron transport due to Horton-ETG model.¹² The system of core transport Eqs. (1) and (2) are highly non-linear and stiff due to the strong dependence of the fluxes on the gradients of the density and temperatures. A nested-iterations based implicit solver is implemented in FACETS to evolve this set of equations.¹³

FACETS incorporates the fluid edge code UEDGE (Refs. 14 and 15) to solve the edge plasma equations. UEDGE includes full single- or double-null x-point geometry with a simulation domain including the region spanning well inside the separatrix and extending to the outer wall and the divertor plate region. A reduced set of the Braginskii transport equations is solved. Usually, the cross diffusion terms are turned off and the Alfvén waves are suppressed by not evolving the induction equation for the magnetic field. Additional assumptions are used to express the equations in a form more amenable to selecting physics terms to either allow faster solution times or to allow better physics under-

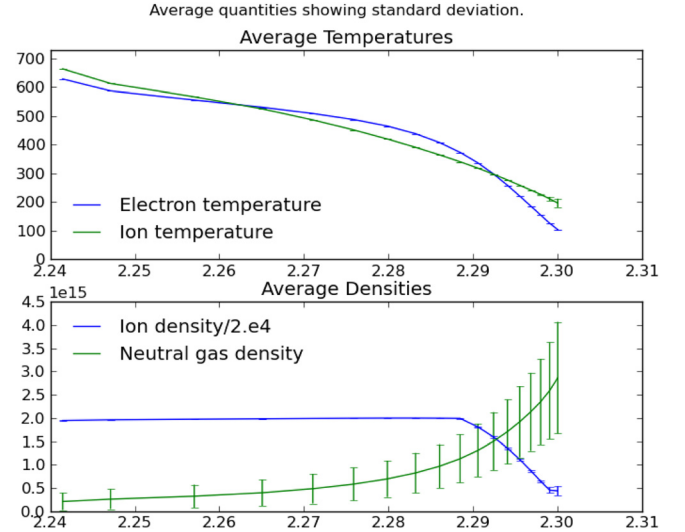


FIG. 1. (Color online) The profiles of the electron and ion temperatures, the plasma density, and the neutral gas density are plotted in the closed field line region from $\psi_N = 0.85$ to the separatrix with the outboard radial distance as the flux coordinate. The error bars correspond to the standard deviation of the quantities along the flux surface. This figure shows that plasma temperatures and density have little poloidal variation at the core-edge coupling point, justifying the use of a flux-surface averaged model. Note, however, that the neutral gas density, not evolved in the core, is not poloidally uniform as the coupling interface is approached.

standing. The specific form of the equations are found in Ref. 15.

For the coupling to be valid, it is necessary the solutions to the edge equations asymptote to the core equations. At a minimum, this means that the plasma quantities are 1D quantities at the CE boundary. In Figure 1, the profiles for the electron and ion temperature, ion density, and neutral gas density from a UEDGE solution are shown for the H-mode plasma discussed in Sec. III. The region plotted is in the closed field line area from a normalized poloidal flux, ψ_N , value of 0.85 to the separatrix, with the outboard radius used as a flux coordinate. As shown, the neutral gas density never equilibrates on a flux surface. This shows the need to keep poloidal variations of the neutrals in the core. However, our core solver currently does not handle this situation.

The electron temperature equilibrates rapidly. Although the plasma density and ion temperature equilibrate more slowly, they are still equilibrated within 1 cm of the separatrix. Because of this, we could take the CE boundary much closer to the plasma edge, but for all of the simulations discussed, we keep it at $\psi_N = 0.85$.

The coupling between the core and the edge regions is performed using an explicit scheme. There are several challenges in setting up a self-consistent problem across the one-dimensional predictive core region with the two-dimensional interpretive edge region. First, the initial profiles and their fluxes need be to continuous across the CE interface; i.e., both the density, temperature, and their derivatives must be continuous. Second, the transport coefficients at the CE interface need to match. This is particularly difficult as completely different models are used to compute the fluxes in the core and edge solvers. An *ad-hoc* scheme is presently implemented in FACETS to enforce this. The continuity in the

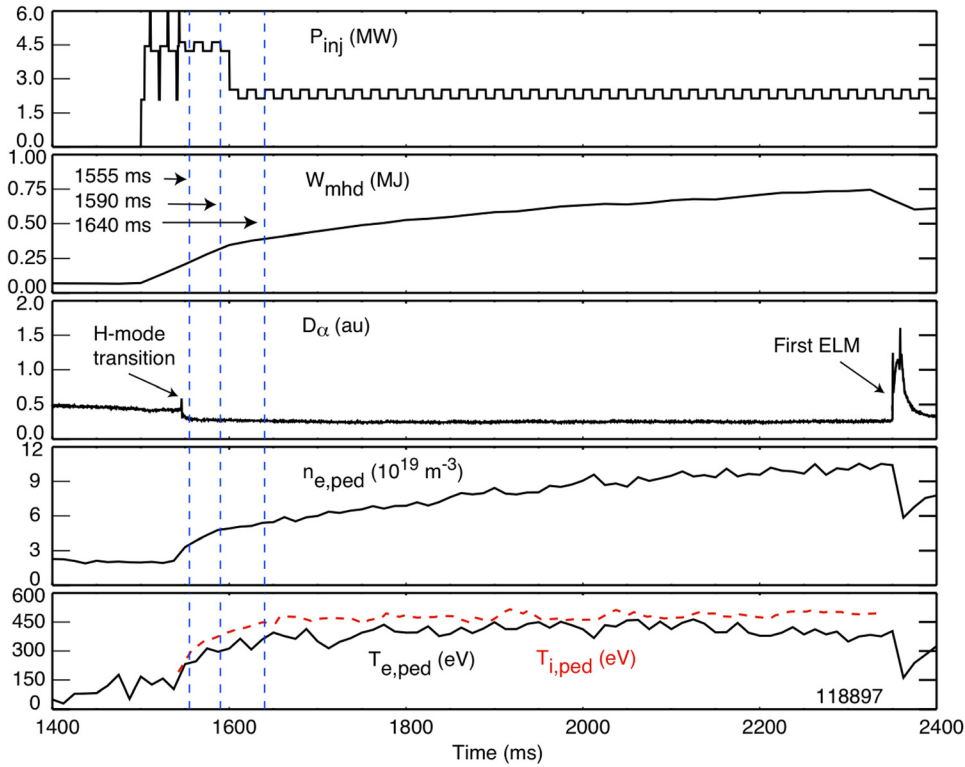


FIG. 2. (Color online) Waveforms for DIII-D shot 118897 shows the time over which the simulation is performed. The neutral beam power (a) raises the stored energy (b). The D_α signal (c) indicates the transition to H-mode and the first ELM occurrence. The density (d) and temperatures (e) at the top of the pedestal shows the formation that occurs.

initial conditions is ensured by using the same set of experimental data to initialize both the core and the edge. However, this does not guarantee the continuity of gradients at the CE interface as two components use different grids and discretization schemes. To solve this problem, a transition from the predictive core fluxes to the interpretive edge fluxes is performed. This is discussed in Sec. III.

A coupled simulation is run as follows. The core and edge components are run concurrently for a specified time-step dt . Typically, both components need to sub-cycle to evolve their solutions by this time-step. The particle and energy fluxes are passed from the core to the edge, i.e., $F^{\rho V} / A = F^{\rho} / \langle |\nabla \rho| \rangle$ is sent to the edge, where A is the area of the flux surface at the CE interface and the angular brackets indicate flux surface averaging. The flux-surface aver-

aged temperature and number density are passed from the edge to the core. These steps are repeated and the simulation evolved in time.

The explicit coupling scheme described above is stable as long as sufficiently small time-steps are taken. Numerical experiments show that a time-step on the order of several $100 \mu\text{s}$ can be taken without the coupled solution going unstable. A fully implicit coupling scheme, although not used in this paper, is also implemented in FACETS and presently being tested for use in core-edge simulations.

III. PROBLEM SETUP AND RESULTS

High-performance tokamak plasma discharges (so-called “H-mode” plasmas) are characterized by steep gradients of

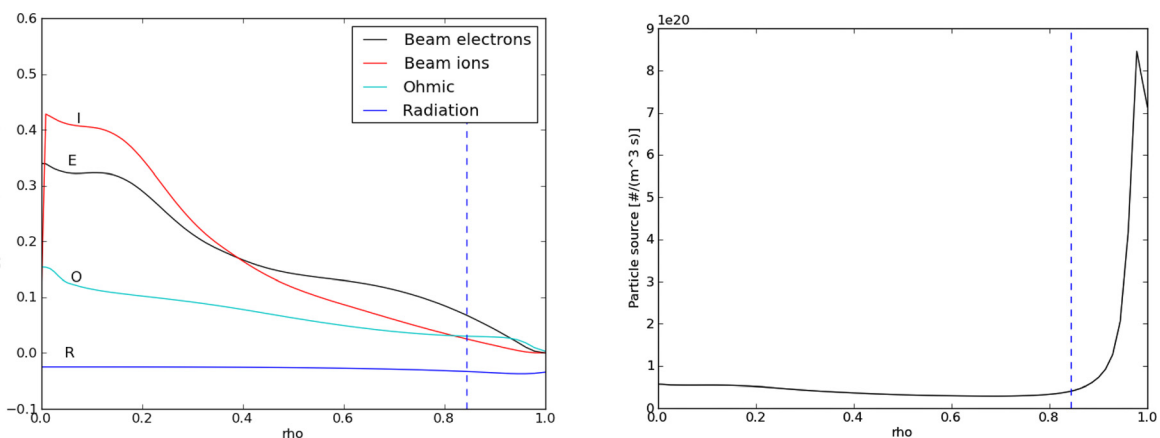


FIG. 3. (Color online) Power sources for electrons and ions (left) and plasma particle source (right). The dashed line indicated the location of the core-edge coupling. Total beam power for ions (I) is 1.78 MW, for electrons (E) 2.21 MW and Ohmic heating (O) is 0.93 MW and radiation loss (R) is 0.40 MW. Net particle injection rate is $2.12 \times 10^{21} \text{ s}^{-1}$. Out of these, the fraction of particles into the core is $4.99 \times 10^{20} \text{ s}^{-1}$. Rest ($1.617 \times 10^{21} \text{ s}^{-1}$) should be accounted for in the edge.

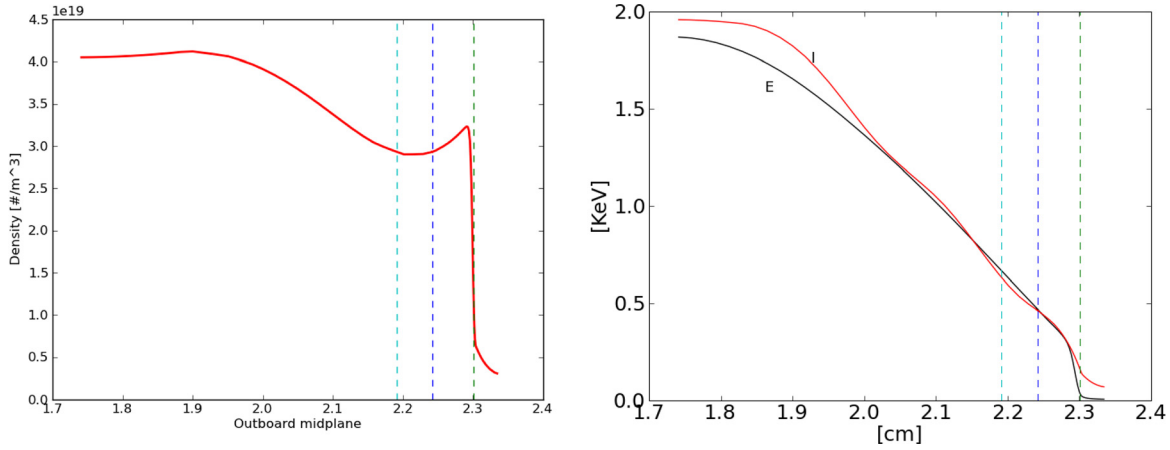


FIG. 4. (Color online) Initial density (left) and temperature (right) profiles for electrons (black, E) and ions (red, I) for shot 118897 at 1555 ms. The blue dashed lines (left) indicate the core-edge interface, the green dashed line (middle) the separatrix and the cyan line (right) the start of transition from predictive to interpretive fluxes.

temperature and density near the plasma separatrix. This region is referred to as the “H-mode pedestal.” Experiments and core transport simulations indicate that core profiles in the H-mode regime have a gradient that is set by the stiff transport caused by turbulence. The overall values of the profiles depend then on the boundary condition to the core region. Thus, the overall fusion gain depends sensitively on the parameters at the top of the pedestal temperature and density.¹⁶ The pedestal height serves as a boundary condition to the core plasma region. As a first test of the FACETS code, we have undertaken the simulation of the pedestal buildup in a particular shot of the DIII-D tokamak. However, due to poor understanding of the edge physics and lack of availability of predictive models for the edge transport, we have used an interpretive analysis to determine the edge cross-field transport coefficients. These are held constant throughout the simulation. Although not fully self-consistent, this serves to test the methodology, give insight into the time-scales over which edge transport coefficients evolve and isolate various physical effects. Future work will address these assumptions.

Coupled core-edge simulations using the methods described in Sec. II are performed to study the pedestal buildup in the DIII-D tokamak. For this, we have chosen to simulate the time slice from 1555 to 1590 ms of DIII-D shot 118897 (Fig. 2). From the experimental waveforms (Fig. 2), it is seen that the neutral beams are turned on around 1490 ms and the plasma density increases from around $2.8 \times 10^{19} \text{ m}^{-3}$ to $3.9 \times 10^{19} \text{ m}^{-3}$. The beam power in the chosen interval averages to around 4.5 MW and eventually drops down to 2.5 MW around 1600 ms. The discharge is ELM free until around 2355 ms.

Beam sources are held constant during the simulation and are taken from an interpretive ONETWO simulation. See Fig. 3 for beam source heating and particle profiles for ions and electrons. The beam adds sources to both the energy as well as density equations. As seen in the figure, part of sources is deposited in the region beyond the core-edge coupling at $\rho > 0.85$. This fraction should be accounted for in the edge, although it is ignored in the simulations presented in this paper.

The simulation is initialized using experimental data averaged around 1555 ms into the discharge. See Fig. 4 for initial density and temperature profiles. The core component is run to $\rho = 0.85$ and the edge component from there to the wall. Note that this puts the pedestal inside the edge component. The reasons for doing this are that the core transport models do not work very well for $\rho > 0.85$ and, we want to ensure that the edge is sufficiently inside the separatrix for the solutions to be relaxed along the poloidal direction.

An initial set of calculations using experimental profiles and sources is performed to determine the cross-field diffusivities from an interpretive UEDGE run. See Fig. 5. The diffusivities drop down significantly in the pedestal to create a transport barrier for the pedestal formation. Once these diffusivities were determined, they were held constant through the 35 ms simulation time.

The core and edge components were evolved using the explicit coupling scheme described above. A time-step of

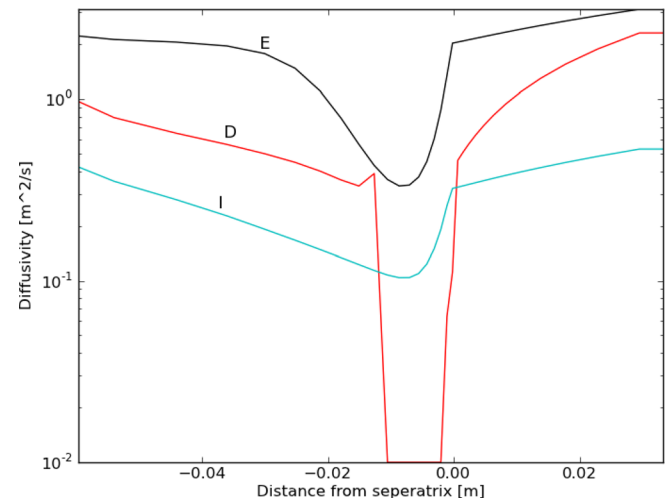


FIG. 5. (Color online) UEDGE diffusivities from interpretive calculations. Red (D) line, black (E) line χ_e , and blue (I) line χ_i . The sudden drop in the diffusivities, specially in D , comes about from the transport barrier needed in the formation of the pedestal. These diffusivities are held constant in the simulations performed in this paper.

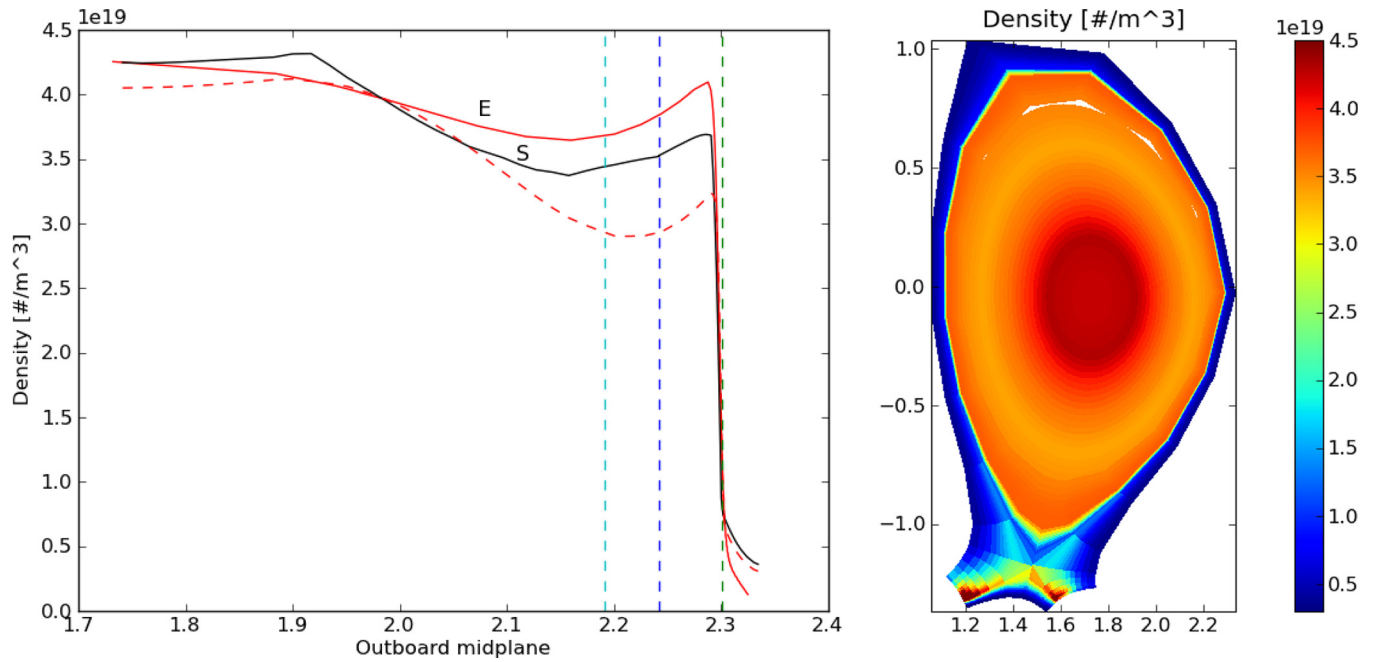


FIG. 6. (Color online) Final experimental (red, E) and simulation results (black, S) for plasma density. The red dashed line shows the initial profile. The density is seen to increase but does not reach the experimentally measured value. Tuning the gas puff to supply an additional fueling source can lead to higher density buildup at the pedestal as shown later in the paper. The 2D plot shows the poloidal variation in the edge.

200 μs was used to couple the components, although the components internally were allowed to choose their own time-steps. Plasma density and electron and ion energy equations were evolved. See Figs. 6–8 for comparison between simulation results and experimental profiles averaged around 1590 ms into the discharge. Our results show that the electron temperature is predicted better than the ion temperature. As seen in the figure, the ion pedestal temperature rises beyond that seen in the experiment, indicating a greater flow of ion thermal energy into the edge. It is also

seen that the density buildup in the edge is under-predicted. One reason for this is that even though an interpretive analysis was used to initialize UEDGE, this analysis is not strictly valid when the coupled system is evolved. The plots also show the 2D poloidal variations of the density and temperatures in the edge. Strong poloidal variations are seen specially in the density near the x-point and the divertor plates. The 2D plots also show the coupling between the 1D core (projected onto a poloidal grid for visualization purposes) and the 2D edge.

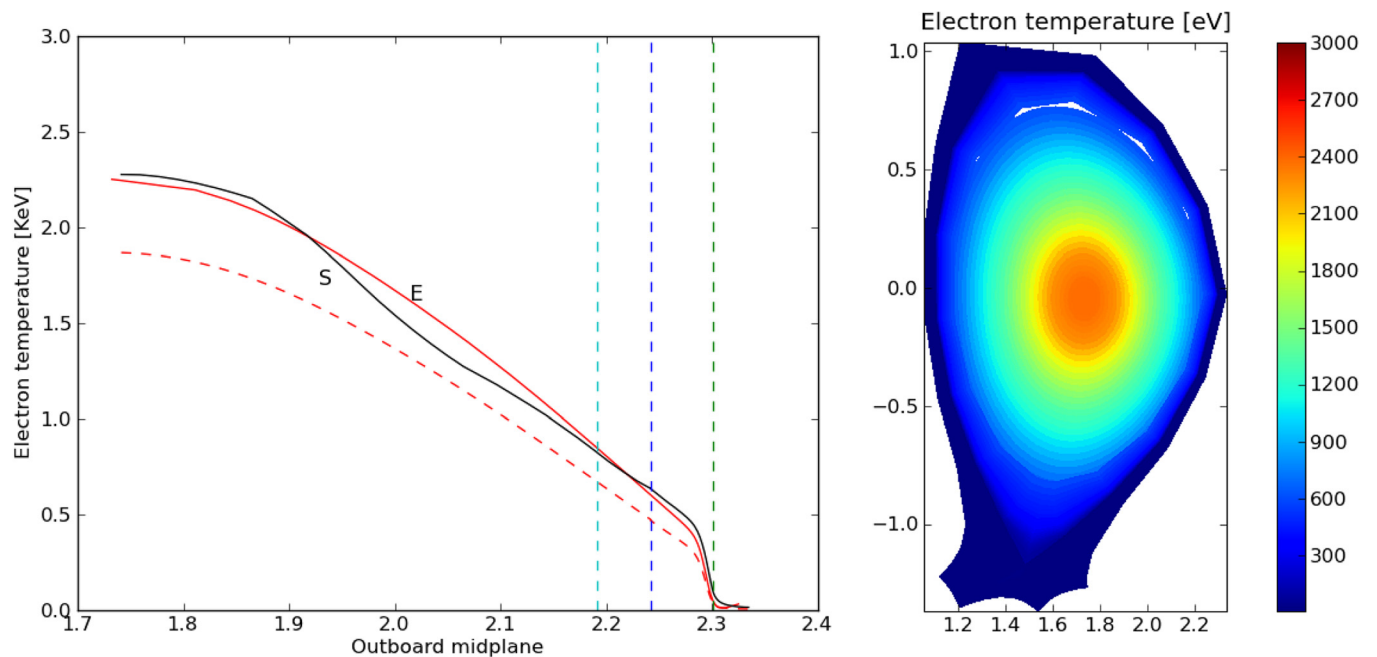


FIG. 7. (Color online) Final experimental (red, E) and simulation results (black, S) for electron temperature at 35 ms. The red dashed line shows the initial profile. The electron temperature compares well with the experimental results. The 2D plot shows the poloidal variation of the electron temperature in the edge.

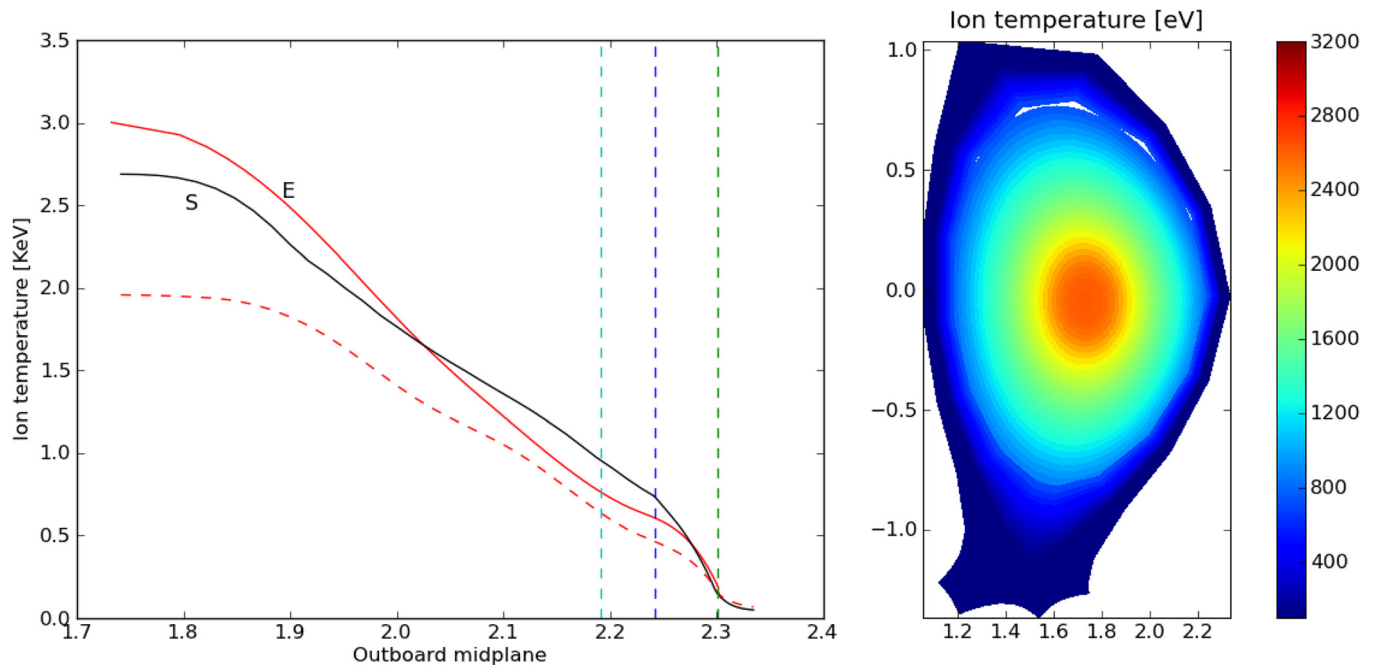


FIG. 8. (Color online) Final experimental (red, E) and simulation results (black, S) for temperature at 35 ms. The red dashed line shows the initial profile. The ion temperature is over-predicted at the pedestal but under-predicted at the axis. The 2D plot shows the poloidal variation of the ion temperature in the edge.

IV. EFFECT OF GAS-PUFF SOURCE ON PROFILE EVOLUTION

The effect of neutral fueling is investigated in this section. To do this, we vary the gas-puff source in the edge region by specifying the neutral source in equivalent amperes. The interpretive UEDGE analysis was performed with 250 A of gas-puff. To study the effect of the gas-puff on the profile evolution, we varied its strength, keeping the cross-field diffusivities in the edge constant. This procedure, although not fully consistent, shows the impact on profile evolution assuming that the edge transport does not change dramatically with small changes in the plasma profile.

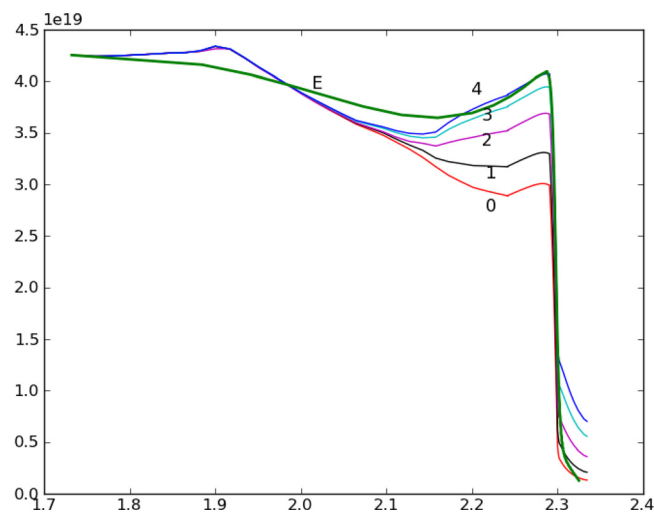


FIG. 9. (Color online) Density profile variation with different gas-puff strength specified as equivalent amperes. The different lines are as follows. Red: 0; no gas-puff, black: 100, magenta: 250, light-blue: 400, and blue: 500. The dark green line (E) is the experimentally measured density profile. The pedestal density increases linearly with the gas-puff strength but, in the simulation time-scale, does not penetrate deep into the core.

Lacking a predictive edge model, this is the best that can be currently accomplished.

Fig. 9 shows the effect of diffusivities gas-puff strength on the plasma density evolution. As expected, it is seen that increasing the amount of neutral fueling in the edge has a direct impact on the pedestal density. The corresponding impact on the electron temperatures is show in Fig. 10. From the figures, it also clear that additional neutral influx has relatively weak effect on the pedestal width and plasma density profiles in the plasma core. This FACETS finding for the pedestal width scaling is in agreement with recent studies of other DIII-D discharges using the SOLPS code.¹⁷

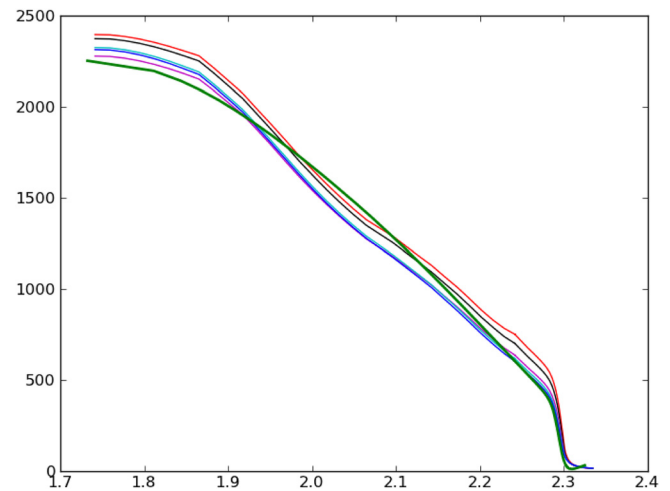


FIG. 10. (Color online) Electron temperature profile variation with different gas-puff strength specified as equivalent amperes. The different lines are labeled as in Fig. 9 and are as follows. Red: no gas-puff, black: 100, magenta: 250, light-blue: 400, and blue: 500. The dark green line is the experimentally measured electron temperature profile. Corresponding the increasing density in the pedestal, the electron temperature decreases as the gas-puff does not add any energy into the plasma but is simply a particle source.

V. CONCLUSIONS

We have presented coupled core-edge simulations of pedestal buildup in a selected shot of the DIII-D tokamak. These calculations show the ability of the framework to perform concurrent coupled simulations with multiple components and serve as a test for the explicit coupling algorithms.

Our initial simulations show that FACETS can evolve the plasma density in addition to the electron and ion energy equations self-consistently using coupled core-edge simulations. Our calculations have shown a sensitivity of the pedestal buildup on the core-edge power balance and also to the presence of a gas-puff as a fueling source in the edge. We expect improvements in the predicted ion temperature and plasma density with a better accounting of the shear flow profiles and a proper tuning of the gas-puff. We believe that our agreement with experiments is reasonable given the uncertainties in the core density transport models, uncertainties in the edge fueling, and the lack of a predictive edge model.

We have also demonstrated that the increase of neutral influx to the level that exceeds the level of neutral influx obtained from analysis simulations with the UEDGE code by a factor of two results in increased plasma density pedestal heights and plasma density levels in the scrape-off-layer region. However, the additional neutral influx has relatively weak effect on the pedestal width and plasma density profiles in the plasma core for the DIII-D discharge studied in this research. This FACETS finding for the pedestal width scaling is in agreement with recent studies of other DIII-D discharges using the SOLPS code.¹⁷

ACKNOWLEDGMENTS

The authors would like to thank to Dr. Lois McInnes and Dr. Hong Zhang for help with the UEDGE code. This

work was partially supported by the US DOE under DE-FC02-07ER54907, DE-AC52-07NA27344, and DE-FC02-04ER54698.

- ¹H. Grad and J. Hogan, *Phys. Rev. Lett.* **24**, 1337 (1970).
- ²S. P. Hirshman and S. C. Jardin, *Phys. Fluids* **22**, 731 (1979).
- ³A. Pankin, G. Bateman, A. H. Kritiz, D. McCune, and R. Andre, *Comput. Phys. Commun.* **159**, 157 (2004).
- ⁴E. F. Jaeger, L. A. Berry, E. F. D. Azevedo, R. F. Barrett, S. D. Ahern, D. W. Swain, D. B. Batchelor, R. W. Harvey, J. R. Myra, D. A. D'Ippolito, C. K. Phillips, E. Valeo, D. N. Smithe, P. T. Bonoli, J. C. Wright, and M. Choi, *Phys. plasmas* **15**, 072513 (2008).
- ⁵G. M. Staebler, J. E. Kinsey, and R. E. Waltz, *Phys. Plasmas* **12**, 102508 (2005).
- ⁶C. S. Chang and F. L. Hinton, *Phys. Fluids* **29**, 3314 (1986).
- ⁷B. Braams, Ph.D. dissertation, University of Utrecht, Netherlands, 1986.
- ⁸G. D. Porter, R. Isler, J. A. Boedo, and T. D. Rognlien, *Phys. Plasmas* **7**, 3663 (2000).
- ⁹G. D. Porter, S. L. Allen, M. R. Brown, M. E. Fenstermacher, D. N. Hill, R. Jong, A. W. Leonard, D. Nilson, M. E. Rensink, and T. D. Rognlien, *Phys. Plasmas* **3**, 1967 (1996).
- ¹⁰J. R. Cary, J. Candy, R. H. Cohen, S. Krasheninnikov, D. C. McCune, D. J. Estep, J. Larson, A. D. Malony, A. Pankin, P. H. Worley, J. A. Carlsson, A. H. Hakim, P. Hamill, S. Kruger, M. Miah, S. Muzsala, A. Pletzer, S. Shasharina, D. Wade-Stein, N. Wang, S. Balay, L. McInnes, H. Zhang, T. Casper, L. Diachin, T. Epperly, T. D. Rognlien, M. R. Fahey, J. Cobb, A. Morris, S. Shende, G. W. Hammett, K. Indireskumar, D. Stotler, and A. Y. Pigarov, *J. Phys.: Conf. Ser.* **125**, 012040 (2008).
- ¹¹J. E. Kinsey, G. M. Staebler, and R. E. Waltz, *Phys. Plasmas* **12**, 052503 (2005).
- ¹²T. Rafiq, A. Y. Pankin, G. Bateman, A. H. Kritiz, and F. D. Halpern, *Phys. Plasmas* **16**, 032505 (2009).
- ¹³A. Y. Pankin, A. Pletzer, S. Vadlamani, J. R. Cary, A. Hakim, S. E. Kruger, M. Miah, T. D. Rognlien, S. Shasharina, G. Bateman, A. H. Kritiz, and T. Rafiq, *Comput. Phys. Commun.* **182**, 180 (2010).
- ¹⁴T. D. Rognlien, J. Milovich, M. E. Rensink, and G. D. Porter, *J. Nucl. Mater.* **196**, 347 (1992).
- ¹⁵T. D. Rognlien, D. D. Ryutov, N. Mattor, and G. D. Porter, *Phys. Plasmas* **6**, 1851 (1999).
- ¹⁶J. Kinsey, G. Staebler, and R. Waltz, *Fusion. Sci. Tech.* **44**, 763 (2003).
- ¹⁷J. Canik, L. Owen, R. Groebner, T. Osborne, C. Lasnier, A. Leonard, J. Watkins, and E. Uterberg, in *13th International Workshop on H-mode Physics and Transport Barriers* (Oxford, UK, 2011), p. 65.